Chapter 9
Simulation: Dropwise Condensation of Water

Basant Singh Sikarwar, Praveen Somwanshi, K. Muralidhar, and Sameer Khandekar

Nomenclature

C_p	Specific heat at constant pressure, W/kg K
h_{lv}	Latent heat of vaporization, J/kg
h	Heat transfer coefficient, W/m^2 K
k	Thermal conductivity of the condensate, W/m K
N	Number of nucleation sites, cm^{-2}
r	Radius of drop, m; suffix b is for base radius
r_{cap}	Capillary length, $\sqrt{\sigma/g(\rho_1 - \rho_v)}$, m
r_{crit}	Size of the drop at instability due to slide-off, m
r_{max}	Size of the drop at instability due to fall-off, m
r_{min}	Radius of thermodynamically smallest drop, m
T	Temperature, K; subscripts w and sat are for wall and saturation
$\Delta T, (T_{sat} - T_w)$	Temperature difference between the saturated vapor and condensing wall, K

Dimensionless Quantities

Ja   Jakob Number, $(C_p/h_{lv})_{ref}(T_{sat} - T_w)$
Nu   Nusselt number, $h r_{cap}/k$
Pr   Prandtl number

Greek Symbols

α	Inclination angle of the substrate from horizontal, radians
θ	Contact angle, radians or degrees; adv, rcd and avg are advancing, receding and average angles
$\Delta\theta, (\theta_{adv} - \theta_{rcd})$	Contact angle hysteresis, $^\circ$

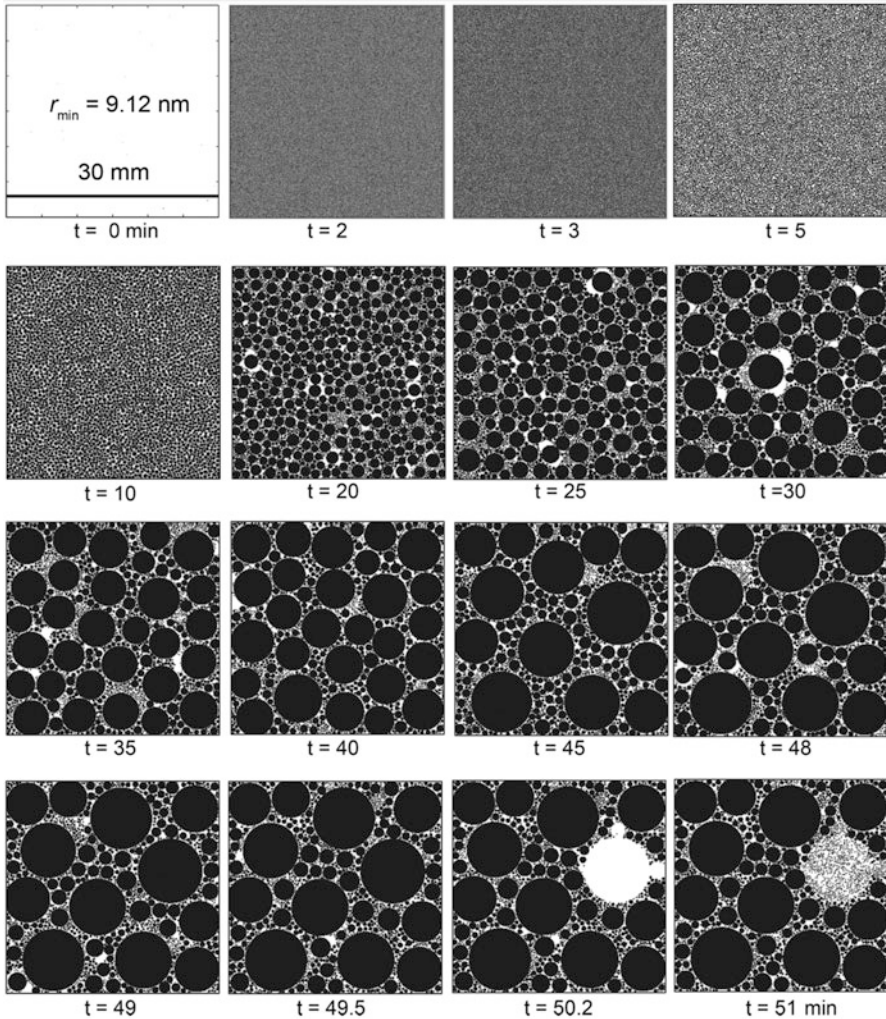## 9.1 Dropwise Condensation of Water Vapor

9.1.1 Effect of Substrate Hydrophobicity

The effect of the hydrophobicity of the substrate towards the condensing liquid is examined in Figs. 9.1, 9.2 and 9.3. Here, drop distribution at selected time instants is pictorially depicted from initial nucleation to the first instance of drop fall-off. Water vapor condenses at 303 K underneath the surface and the degree of subcooling is 5 K. The substrate is horizontal and various contact angles are considered.

Figure 9.1 shows a time sequence of condensation patterns for a contact angle of 90°. Drop diameter at criticality is 4.63 mm and fall-off first occurs at 50.15 min after commencement of condensation. Figure 9.2 shows the corresponding spatio-temporal drop distribution for a contact angle of 120°. Drop diameter at criticality is 3.088 mm and fall-off first occurs at 21.55 min after commencement of condensation. Figure 9.3 shows the spatio-temporal drop distribution for a contact angle of 140°. Drop diameter at criticality is 2.14 mm and fall-off first occurs at 7.25 min after commencement of condensation.

As can be seen, a reduction in wettability increases the contact angle and leads to a smaller base circle of the drop and, therefore, smaller surface forces retaining the drop against gravity. Thus, two effects are clearly visible: (a) The droplet volume at the time of fall-off is smaller (Figs. 9.1, 9.2, and 9.3); (b) with increasing contact angle, the drops achieve fall-off criticality earlier in the cycle.

The area of coverage by drops for various contact angles is shown in Fig. 9.4a. The hydrophobicity of substrates decreases the area of coverage. Therefore, highly hydrophobic substrates (higher contact angle) have higher available exposed nucleation sites density at any given time of condensation (Fig. 9.4b). The size and population of maximum diameter drops have a significant impact on dropwise condensation, due to the limitations imposed by the diffusional resistance of the liquid. The effect of substrate hydrophobicity on the surface-averaged heat transfer rate during dropwise condensation is shown in Fig. 9.4c. The apparent contact angles clearly show an effect on heat transfer. The size of the drop at fall-off as well as the time required for fall-off decrease as the hydrophobicity of the substrate increases. All other conditions remaining unchanged, the fall-off time for a pendant drop is seen to be a linear function of the contact angle (Fig. 9.4d).

Fig. 9.1 Drop distribution from the start to the first fall-off during dropwise condensation of water vapor at 303 K with 5 K subcooling underneath a horizontal substrate of contact angle 90°

For a given initial nucleation site density, heat transfer can be increased by having a contact angle higher than the 90°. Accordingly, the substrates having higher hydrophobicity result in the condensate having drop size distributions towards the smaller diameter (Figs. 9.1, 9.2, and 9.3). It results in lowering the overall diffusion resistance offered by the condensing drops. In addition, increased hydrophobicity generates many nucleation sites, at any given time. The nucleation sites available for nucleation are shown in Fig. 9.4b. Initially, it decreases according to a power law but after reaching a dynamic steady-state it varies quasi periodically due to coalescence and fall-off. The frequency of drop fall-off, size of the minimum drop and size of the maximum drops, for substrates having various degree of hydrophobicity, during water vapor condensation are summarized in Table 9.1.
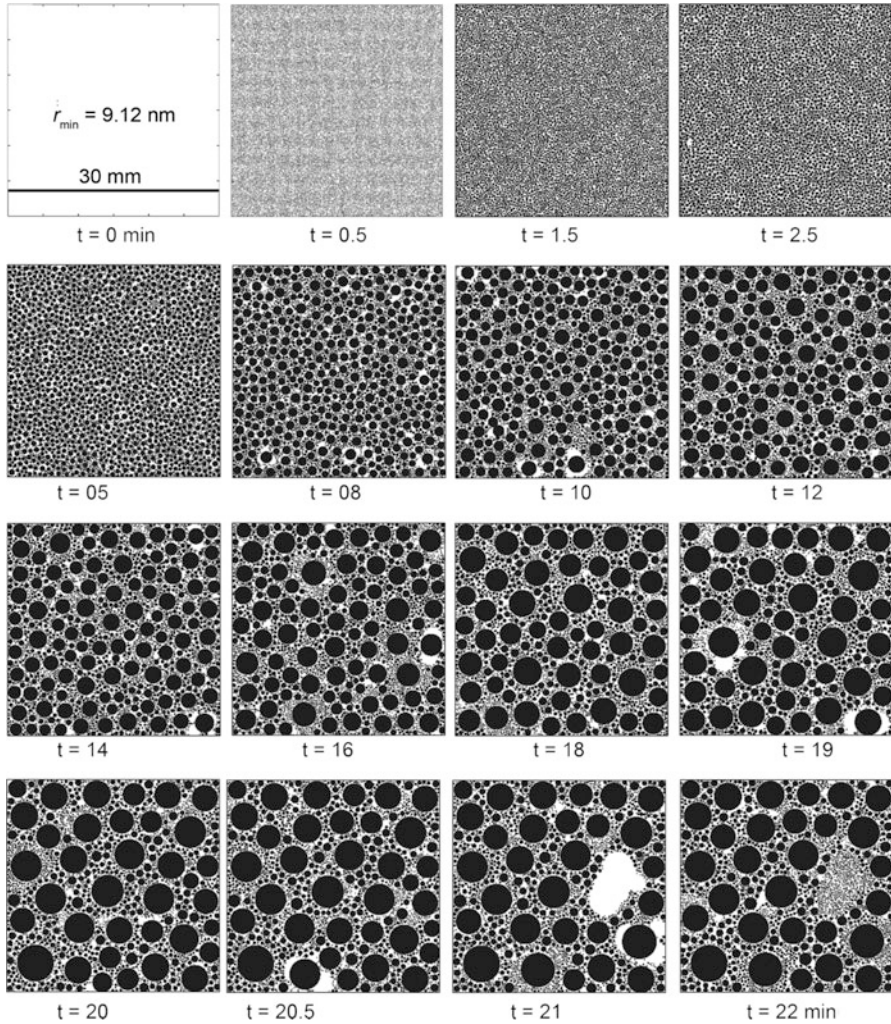
Fig. 9.2 Drop distribution from the start to the first fall-off during dropwise condensation of water vapor at 303 K with 5 K subcooling underneath a horizontal substrate of contact angle 120°

As given in Table 9.1, the substrate hydrophobicity decreases the critical size (of fall-off), hence resulting in a higher population of small drops. Therefore, one concludes that a substrate having a high hydrophobicity with the condensate fluid is desirable in dropwise condensation. Figure 9.5a shows the frequency (namely, the number of drops) as a function of the drop radius, 10 min after commencement of condensation for a contact angle of 90°, saturation temperature of 303 and 5 K subcooling. At later times, drops of higher sizes are to be seen. For the present simulation, the fall-off time of the first drop was approximately 50.2 min. Figure 9.5b
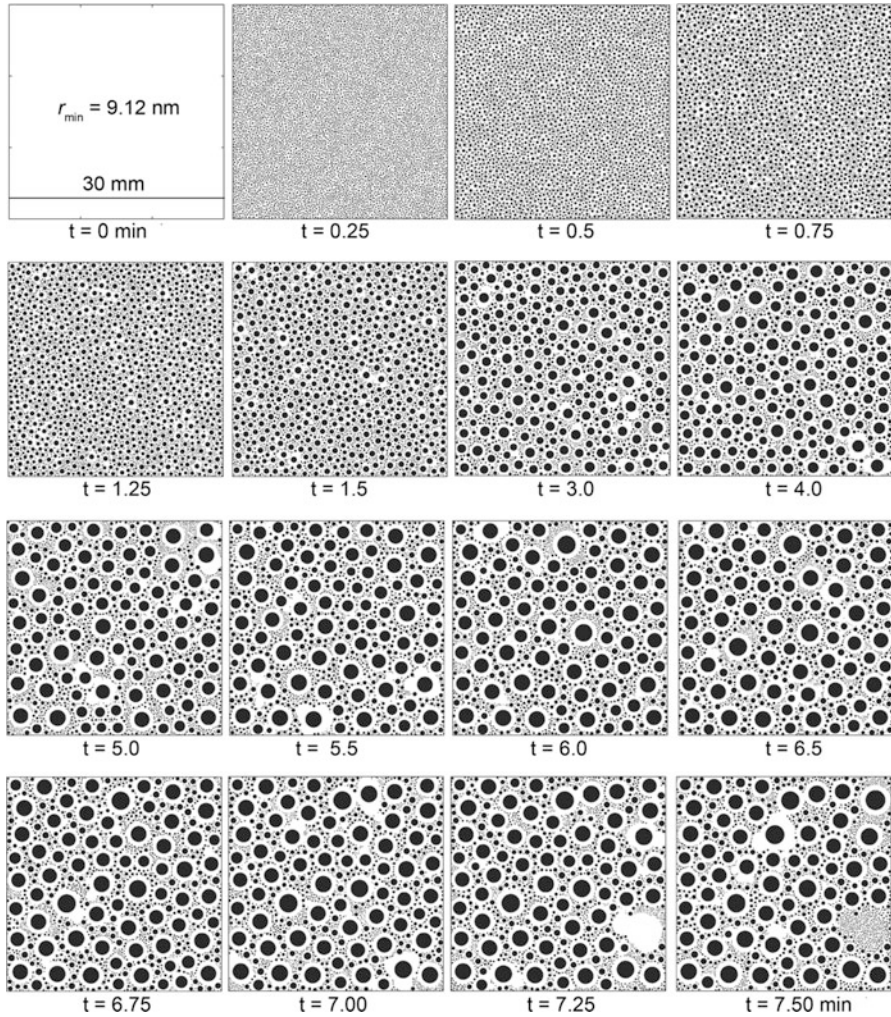
Fig. 9.3 Drop distribution from the start to the first fall-off during dropwise condensation of water vapor at 303 K with 5 K subcooling underneath a horizontal substrate of contact angle 140°

shows that very small droplets nucleate on the substrate at 50 min, immediately before the first drop falls-off at 50.2 min.

9.1.2 Effect of Substrate Inclination

Figures 9.6, 9.7, and 9.8 show the distribution of drops arising from water vapor condensation at 303 and 5 K subcooling from initial nucleation to the first slide-off underneath substrates of various orientation (30°, 60°, and 90°). The pictorial views
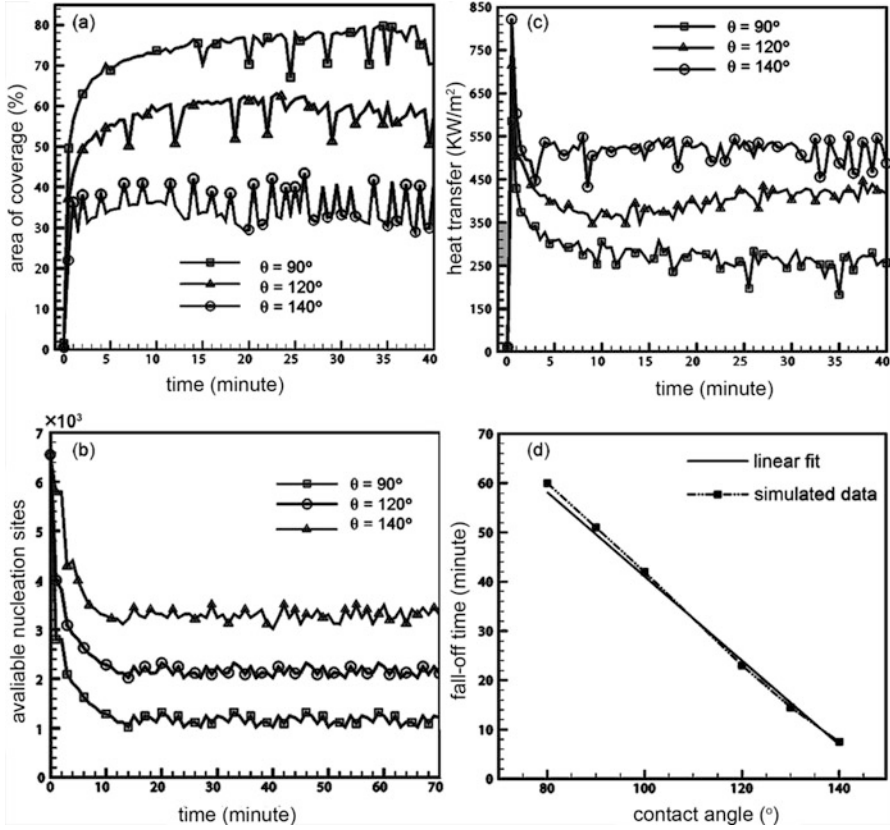
Fig. 9.4 (**a**) Area of coverage as a function of time, (**b**) available nucleation sites over the substrate of size 30 × 30 mm with respect to time for various contact angles at 303 K and degree of 5 K subcooling, (**c**) fluctuations in heat transfer rate on a substrate with respect to time and (**d**) fall-off time of a drop as function of the contact angle

Table 9.1 Results summarizing parameters of dropwise condensation of water vapor at 303 and 5 K subcooling after reaching a quasi-steady state

Contact angle (°)	Radius		Initial nucleation sites (cm^{-2})	Available nucleation sites on a 30 × 30 mm area	First fall-off (min)	Frequency (s^{-1})	Heat transfer (kW/m^2)
	r_{min} (mm)	r_{max} (mm)					
90	9.1×10^{-6}	4.64	10^6	1122	50.2	360	270
			10^7	1137	38.5	187	282
120	9.1×10^{-6}	3.08	10^6	1977	21.5	242	395
			10^7	2015	17.8	155	512
140	9.1×10^{-6}	2.14	10^6	3656	7.2	189	525
			10^7	3684	6.7	85	580

Fig. 9.5 (**a**, **b**) Temporal variation in drop size distribution for condensing water vapor underneath a horizontal substrate for contact angle 90°. For clarity, data for 1–10 min are separately plotted from the data for 30–50 min. The fall-off time for the first drop was equal to 50.2 min in this simulation
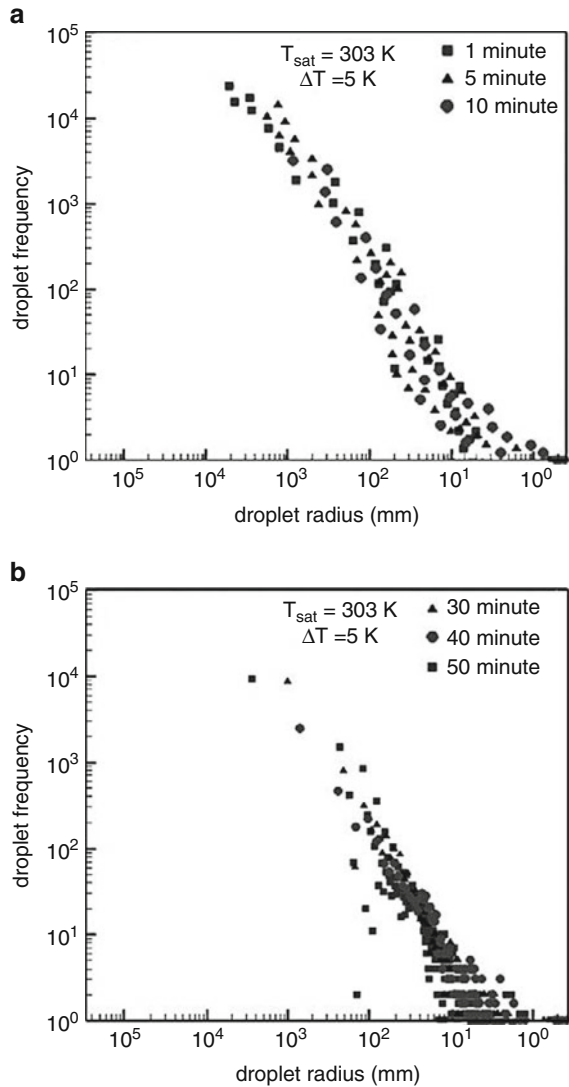
of condensations have site density 10^6 cm^{-2}, substrate size 30 × 30 mm for substrates of inclination 30° and 60° and 20 × 20 mm for an inclination of 90°. For these simulations, the advancing and receding angles are taken as 118.5° and 101.5°, yielding an average contact angle of 110° and a contact angle hysteresis of 17°.

Condensation patterns on various inclinations show broad similarity. The point of difference is the size of the drop at slide-off and the average cycle time for slide-off from the substrate. These quantities decrease as the angle of inclination with respect to the horizontal increases.
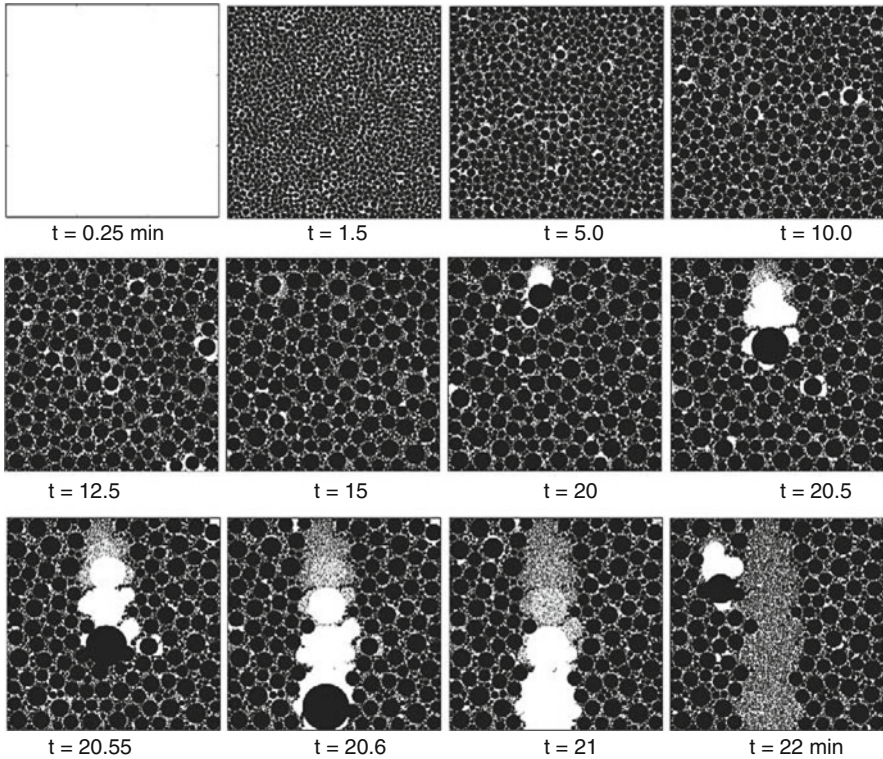
Fig. 9.6 Drop distribution from the start to the first slide-off during dropwise condensation of water vapor at 303 K with 5 K subcooling underneath an inclined substrate. The angle of inclination is 30°, and the size of the substrate is 30 × 30 mm

The variation of the critical size of the droplet with respect to substrate orientation is depicted in Fig. 9.9. The critical drop size decreases with substrate hydrophobicity and inclination, causing a reduction in the cycle time and hence results in more frequent instances of renucleation. The reduction in the cycle-averaged drop size is an important factor in increasing heat transfer from strongly hydrophobic surfaces.

For ease of calculation, the data of Fig. 9.9 is correlated for various surfaces by

$$\frac{r_{\text{crit}}}{r_{\text{cap}}} = \left(2.1612 - 0.7699\theta_{\text{avg}}\right)\left(\Delta\theta\right)^{0.5}\alpha^{-0.4266} \tag{9.1}$$

The correlation coefficient of Eq. (9.1) is 99.8%; it simplifies dropwise condensation calculations within the hierarchical model and considerably reduces the computational time.

The heat transfer coefficient of dropwise condensation for a given saturation temperature and degree of subcooling is dependent on the contact angle, contact angle hysteresis, and substrate orientation, which in turn affect the criticality of
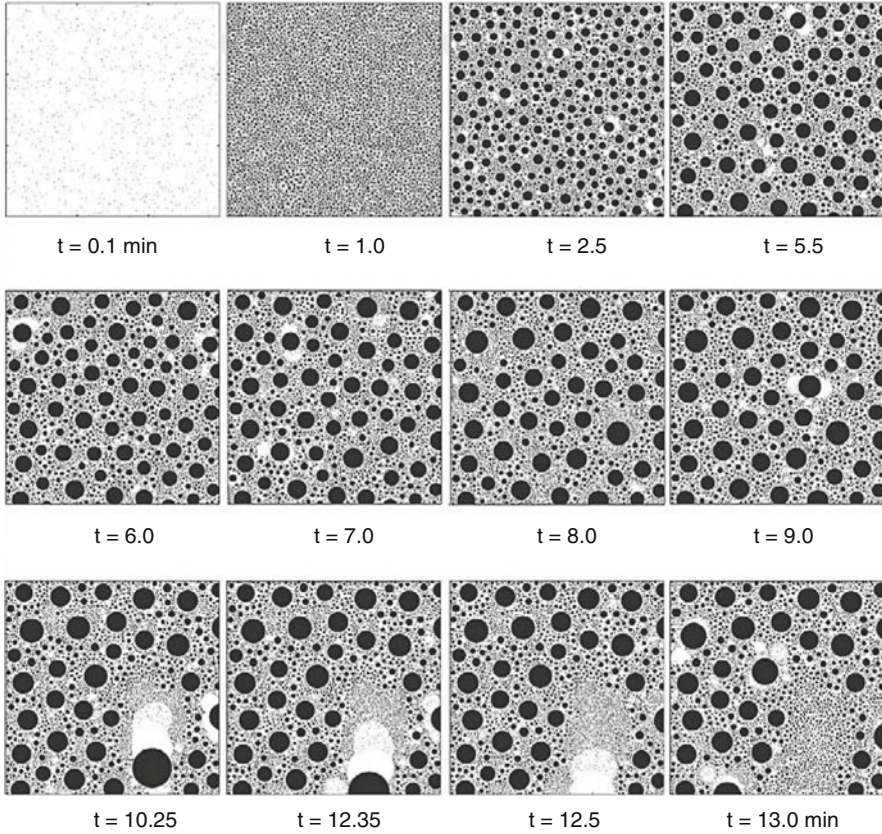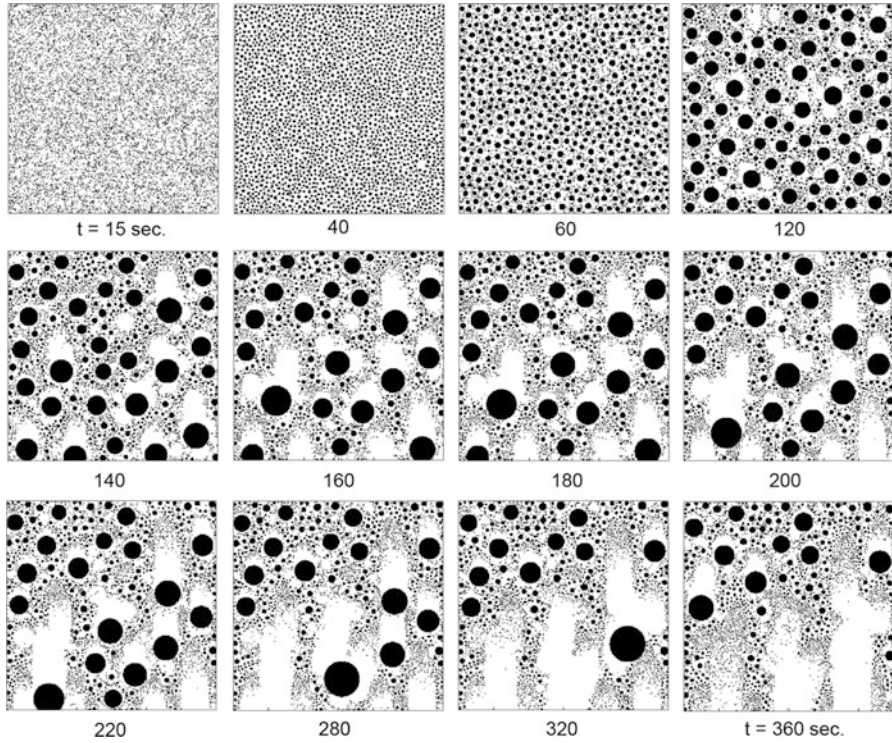
Fig. 9.7 Drop distribution from the start to the first slide-off during dropwise condensation of water vapor at 303 K with 5 K subcooling underneath an inclined substrate. The angle of inclination is 60°, and the size of the substrate is 30 × 30 mm

sliding. The effect of critical radius on heat transfer at 303 and 5 K subcooling is depicted in Fig. 9.10a. It is seen that heat transfer coefficient increases as radius of departure from the substrate decreases. The correlation for heat transfer coefficient is

$$h = 0.19 \, r_{\text{crit}}^{-1.2} \tag{9.2}$$

where h is in unit of MW/m^2 K and r_{crit} is in mm.

Figure 9.10b shows the variation of heat transfer coefficient with respect to the angle of inclination of the substrate. Numerically obtained data of water condensing underneath various inclined (0–90°) substrates is shown for an average contact angle of 110°, contact angle hysteresis of 17° and 5 K subcooling at various saturation temperatures. The result exhibits a heat transfer coefficient for vertical substrate that is 40–50% higher than the horizontal substrate.

Fig. 9.8 Drop distribution from the start to the first slide-off during dropwise condensation of water vapor at 303 K with 5 K subcooling underneath an inclined substrate. The angle of inclination is 90°, and the size of substrate is 20 × 20 mm

Fig. 9.9 Critical base radius of the drop at instability (r_{crit}/r_{cap}) for a pendant arrangement plotted as a function of substrate orientation (α). Contact angle hysteresis is a parameter while the average contact angle is 105°
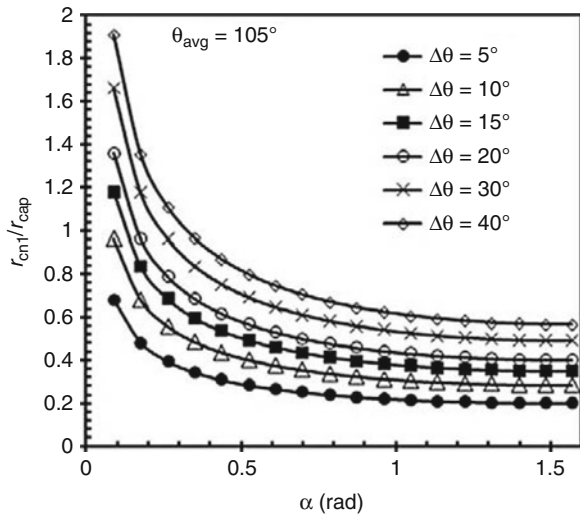
Fig. 9.10 (**a**) Dependence of heat transfer on the departure drop radius. (**b**) Effect of substrate inclination on heat transfer coefficient
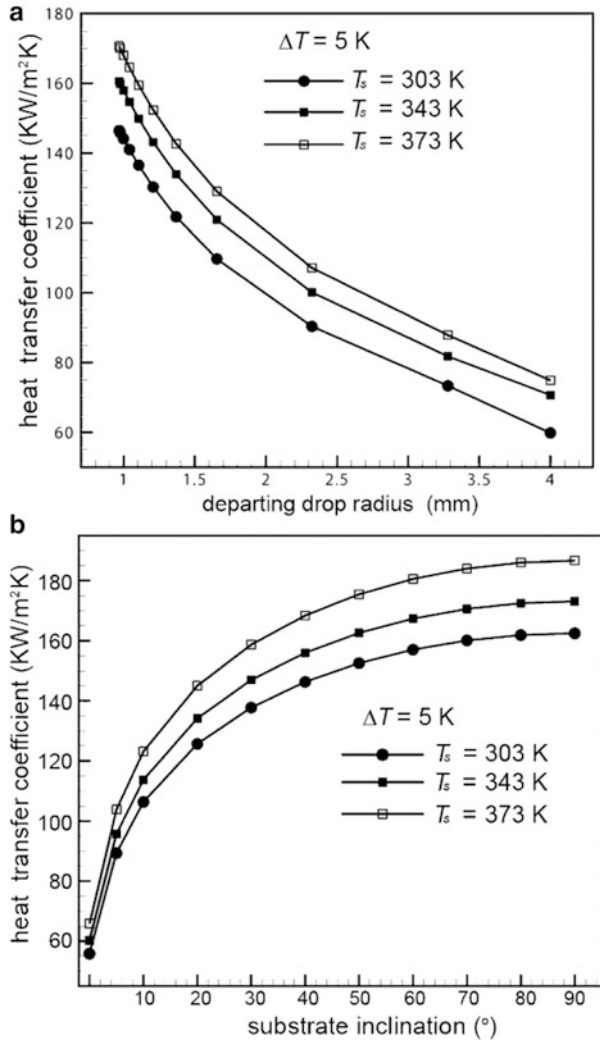
The effect of substrate inclination on the temporal distribution of area coverage of drops is presented in Fig. 9.11a. Inclination of the substrate facilitates easier movement of drops by sliding, leading to a sweeping action. Therefore, the effective steady-state coverage is smaller for inclined substrates, changing from 76.1% for a horizontal substrate, 71.2% for 5° inclination, and 67.4% for the substrate with 10° inclination. At the instant of the first fall-off (for the horizontal substrate) and the first slide-off (for the inclined substrate), Fig. 9.11b depicts the drop size distribution as a function of radius, for various inclination angles. The distribution follows a power law with the negative slope increasing with angle, reflecting the repeated appearance of small drops at fresh nucleation.

Fig. 9.11 Effect of substrate inclination. (**a**) Temporal variation of area coverage of drops during condensation of water in the pendant mode. (**b**) Drop size distribution just before fall-off (for horizontal substrate) or slide-off (inclined substrate). For this simulation, $\theta_{adv} = 118.5°$ and $\theta_{rcd} = 101.5°$. $T_s = 303K$, 5 K subcooling
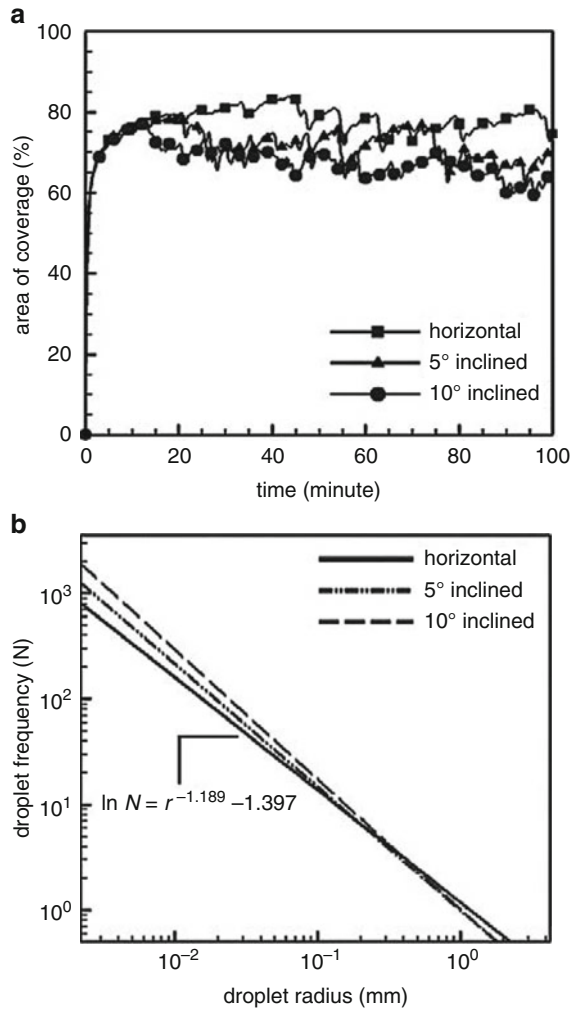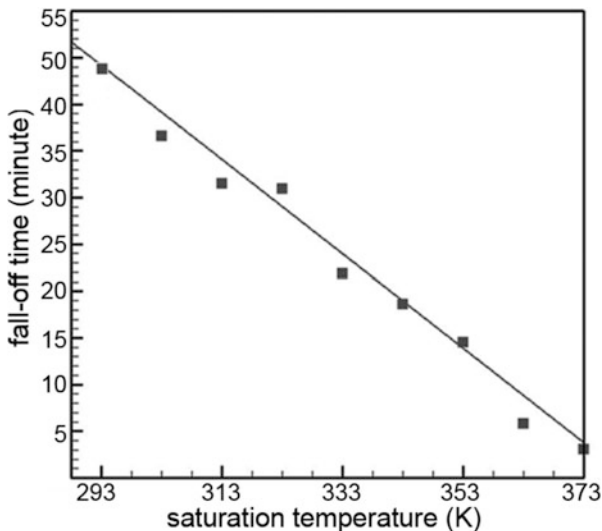

9.1.3 Effect of Saturation Temperature and Subcooling

For a given degree of subcooling ($\Delta T_{sat} = 5$ K), the effect of saturation temperature on drop departure time underneath a horizontal substrate is shown in Fig. 9.12. Increasing the saturation temperature reduces the fall-off time and hence the size of the largest drop, indicating an increase in the overall heat transfer coefficient. The diffusional thermal resistance within the drop is a major limiting factor of condensation heat transfer. Hence, increasing the saturation temperature increases the thermal conductance of the water drop. A marginal increase in the overall resistance is also noticed due to a reduction in the interfacial heat transfer coefficient; it

Fig. 9.12 Variation in drop departure time (time required for first fall-off) on a horizontal substrate with respect to the saturation temperature. Fluid employed is water, 5 K subcooling, contact angle = 110°, nucleation site density = 10^6 cm^{-2}. For a given nucleation site density, the fall time has an uncertainty of ± 3 min, depending on the random assignment of initial droplet centers on the substrate

essentially proves to be inconsequential as the overall thermal resistance is dominated by conduction resistance of the droplet.

Figure 9.13 shows the effect of saturation temperature and degree of subcooling on the heat transfer coefficient of dropwise condensation underneath horizontal and vertical substrates. The data show a tendency of increasing heat transfer coefficient with increasing saturation temperature and degree of subcooling. This is caused mainly by the decrease in the interfacial resistance at high saturation temperature of water vapor.

Increasing the degree of subcooling increases the density of active nucleation sites on the condensing substrate. On the basis of numerical data, the heat transfer coefficient (kW/m^2 K) is empirically correlated with the critical radius of drop (mm), degrees of subcooling and saturation temperature (both in units of °C) for water vapor condensation underneath an inclined substrate with a nucleation site density of 10^6 cm^{-2} by

$$h = (0.42\Delta T + 6.4)T_{\text{sat}}^{0.75}\, r_{\text{crit}}^{-1.18} \qquad (9.3)$$

Here, the critical radius depends on contact angle, contact angle hysteresis, and angle of inclination of substrate with respect to the horizontal. It is preferable to cast this correlation in dimensionless form, applicable for all the inclinations, saturation temperature, and degree of subcooling. The heat transfer correlation for condensation of water vapor underneath an inclined substrate is

Fig. 9.13 Dependence of heat transfer coefficient on saturation temperature and degree of subcooling. (**a**) Horizontal substrate, (**b**) vertical substrate. Condensing fluid is water average, contact angle is 110°, contact angle hysteresis is 17° and nucleation sites density is 10^6 cm^{-2}
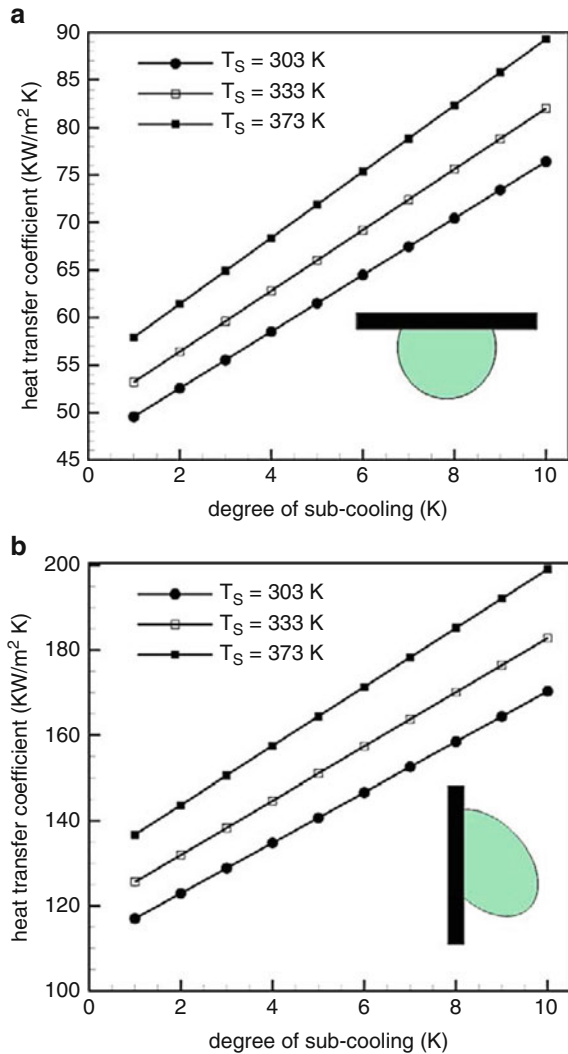
$$\mathrm{Nu} = \left(8.54 \times 10^3\ \mathrm{Ja} + 240\right)\left(\frac{T_{\mathrm{sat}}}{T_{\mathrm{ref}}}\right)^{0.75}\left(\frac{r_{\mathrm{crit}}}{r_{\mathrm{cap}}}\right)^{-1.18} \tag{9.4}$$

Equation (9.4) has a correlation coefficient of 98.5%. Standard reference values used are properties of water at the normal boiling point.
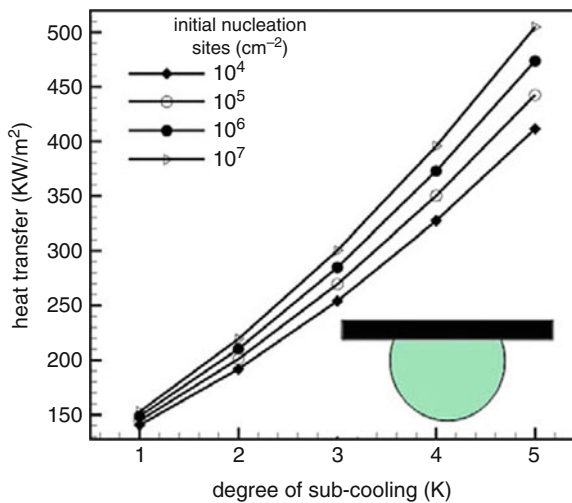
9.1.4 Effect of Nucleation Site Density

Increasing the density of nucleation sites leads to a large overall heat transfer in dropwise condensation. This effect arises mainly from a reduction in the size of the drop before coalescence. Early coalescence allows virgin spaces for new initial drops, causing a high population of small drops. One can conclude that a surface providing a higher nucleation sites is desirable for dropwise condensation. The number of nucleation sites is chosen as a parameter for condensation underneath a horizontal substrate, the working fluid being water. The effect of initial nucleation site density on heat transfer is shown in Fig. 9.14 for a contact angle of 110° and a saturation temperature of 303 K.

As the number of nucleation sites increases per unit area, many small drops nucleate on exposure of the surface to vapor, i.e., the average drop size within a cycle decreases. The conduction resistance is thus lowered, leading to an increase in average heat transfer coefficient.

9.1.5 Effect of Promoter Layer Thickness

Dropwise condensation of water underneath metal surfaces is rarely observed in natural conditions. It is generally promoted with a suitable coating. An understanding of the role of coatings is critical not only because it determines the surface wettability, but it adds an extra thermal resistance. The nucleation density is also dependent on the promoter layer. The mathematical model of the present work is utilized for designing and quantifying the effect of the coating.

Fig. 9.14 Overall heat transfer rate as a function of subcooling with nucleation site density as a parameter

Fig. 9.15 Overall heat transfer as a function of the degree of subcooling with varying thickness of the promoter layer underneath a horizontal substrate. Fluid considered is water at 303 K, contact angle of 100° and nucleation site density of 10^6 cm^{-2}
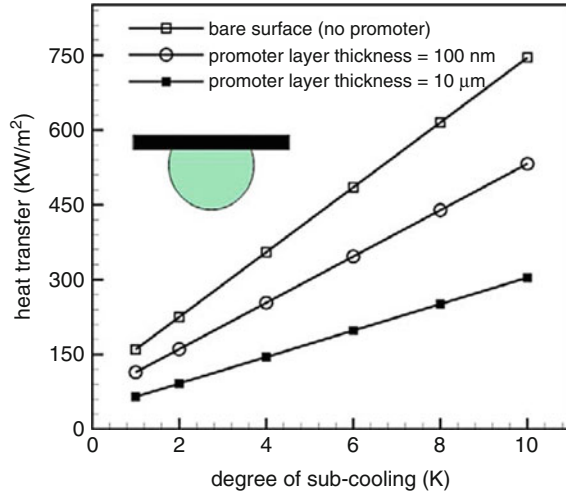
Figure 9.15 presents the overall heat flux for coatings of varying thicknesses. The computation was carried out when the layer with the thermal conductivity of 0.28 W/m K creates a 100° contact angle. The overall heat flux is significantly influenced by the thickness. When the 10 μm thick promoter thickness is reduced to 100 nm without any change in the contact angle and nucleation density, heat transfer improves by a factor of 1.75. If the same hydrophobicity can be achieved without any promoter, the condensing surface can produce 1.4 times the heat transfer of the 100 nm thick promoter and 2.45 times that of the 1 μm promoter, respectively. This result shows that a redundantly thick coating results in a significant degradation of heat transfer.

9.1.6 Effect of Wettability Gradient

The effectiveness of dropwise condensation is improved by moving the liquid drop that grows on or underneath a solid substrate. The droplet moving over the surface wipes other droplets off. Consequently, more unexposed area is available where smaller droplets can form again. This process of wiping and formation of new small droplets exhibits low heat transfer resistance and is the reason for a large heat transfer coefficient.

Literature (Lee et al. 1998; Daniel et al. 2001; Liao et al. 2006; Zhu et al. 2009; Pratap et al. 2008) suggests various ways of controlling the motion of droplets. A simple approach for mobilization of drops is to incline the surface with respect to horizontal, wherein the gravitational body force is responsible for the droplet motion. Alternatively, one can introduce a variation of surface tension gradient on the substrate. Surface tension can be varied as follows: (1) applying a large temperature gradient on the substrate, in which Marangoni effect leads to drop motion and
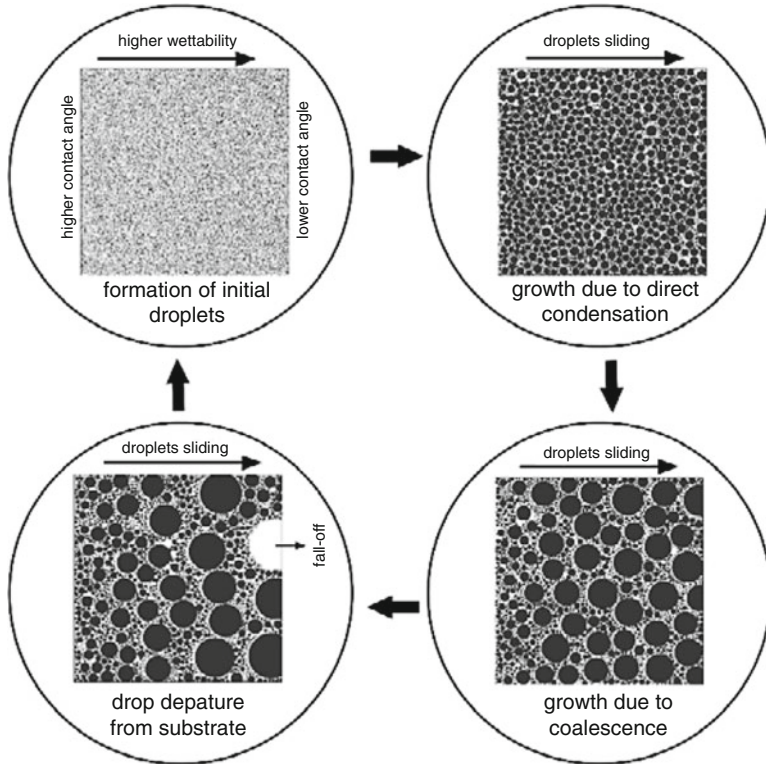
Fig. 9.16 Cycle of dropwise condensation observed in water vapor condensation underneath a horizontal substrate with unidirectional wettability gradient

(2) movement of micro-droplets underneath a horizontal surface by a variable-surface-energy coating, which creates a wettability gradient. To facilitate drop motion by artificially forming a wettability or surface energy gradient on the surface by suitable chemical treatment is a promising technique for drops motion as compared to applying a temperature gradient on the substrate. It is quite possible on copper and glass surfaces by depositing organic long chain monolayers (Subramanian et al. 2005; Pratap et al. 2008).

Daniel et al. (2001) and Bonner (2010) reported from experiments that the condensation on a wettability gradient surface is quite large as compared to a horizontal substrate without wettability gradient. Against this background, dropwise condensation of water underneath a horizontal surface with unidirectional constant wettability gradient is numerically simulated by the mathematical model. Figure 9.16 shows features of the condensation cycle underneath a horizontal substrate with wettability gradient. These are like those of an inclined surface. The points of difference for a graded surface are: (1) drops shift towards the higher wettability side and hence drops of all the sizes are in motion, (2) the velocity of drops depends
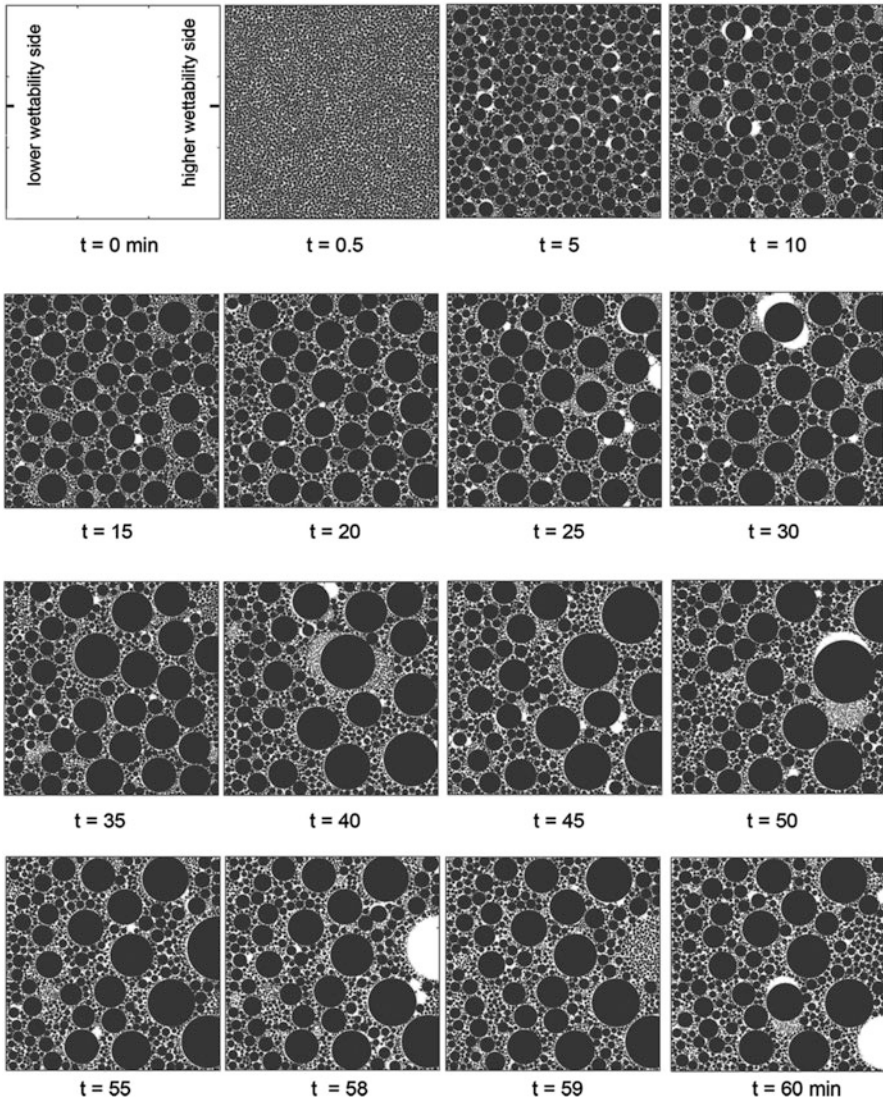
Fig. 9.17 Distribution in drops in dropwise condensation of water vapor underneath a horizontal substrate with wettability gradient $0.33° \text{ mm}^{-1}$. Lower wettability side has a contact angle of $100°$, size of substrate is 30×30 mm, nucleation site density 10^6 cm^{-2} at saturation temperature 303 and 5 K subcooling

on their size and position on the substrate, and (3) growth and sliding occur simultaneously.

Figures 9.17 and 9.18 show the drop distribution from initial nucleation to dynamic steady-state at selected instants of time underneath horizontal substrates
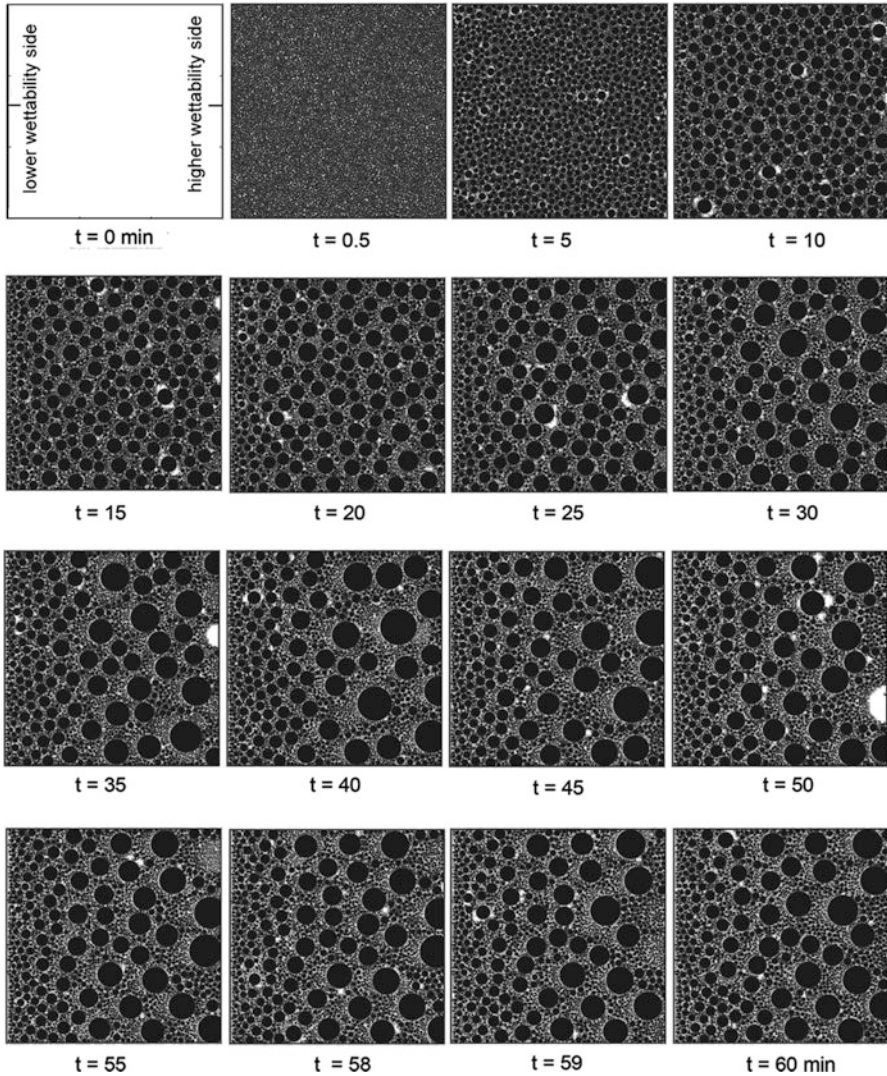
Fig. 9.18 Distribution in drops in dropwise condensation of water vapor underneath a horizontal substrate of wettability gradient 0.33° mm^{-1}. Lower wettability side has a contact angle of 110°, size of substrate is 30 × 30 mm, nucleation site density 10^6 cm^{-2} at saturation temperature 303 and 5 K subcooling

with constant wettability gradient. Figure 9.17 shows a condensation pattern of water vapor at a saturation temperature of 303 and 5 K subcooling underside of substrate having contact angles of 100° and 90°. Figure 9.18 shows the condensation of water vapor at under similar conditions as in Fig. 9.17 but with contact angles of 110° and 100°. In both the surfaces, the wettability gradient is 0.33° mm^{-1}. As drops grow,

they become unstable and move towards the higher wettability side of the substrate. Therefore, on an average, larger drops are present at the higher wettability side. The patterns of drops underneath a wettability gradient follow approximately the same trend as those underneath an inclined substrate. The point of difference is that there is no critical size for drop instability. Every drop becomes unstable due to surface tension difference at the three-phase contact line. Gravity, viscous, and surface tension forces are important to determine the terminal velocity of the drop. Hence, the sliding velocity depends on the size and position of the drop underneath the substrate. Fall-off is observed as a rule, on the higher wettability side of the substrate. Figures 9.17, 9.18, and 9.19 also depict small drops present at the lower wettability side of the substrate. On the higher wettability side, the driving force of drop becomes small, the drop cannot move, and it reaches criticality of fall-off (Fig. 9.17, 58 min). These results reveal that the micro-drop size can be moved as the hydrophobicity of wettability gradient substrate increases.

Figure 9.20 compares dropwise condensation patterns of water vapor underneath horizontal and inclined non-graded substrates with a horizontal graded substrate. Spatial distribution of drops at an instant just before the first drop leaves the surface on a graded substrate, first slide-off from an inclined substrate and the first fall-off from a horizontal substrate, respectively, are compared in Fig. 9.20a.

As wettability gradient induces motion to the drops of every size, there exists an exposed virgin area behind every droplet on the graded substrate, as shown in Fig. 9.20a. Hence, the fraction of total area exposed for fresh condensation tends to be greater for a graded surface when compared to the other two configurations. Figure 9.20b shows the frequency of occurrence of a drop of a given radius, namely the histogram, on the three substrates, at an instant just before slide-off or fall-off criticality is attained. Drops slide-off for a graded surface as well as for the inclined. Drops fall-off from a horizontal surface. From Fig. 9.20b, it is clear that a graded substrate has a larger number of smaller sized drops as compared to the other two. Largest drops are formed on a horizontal substrate before they fall-off. This eventually leads to a slower condensation rate on the horizontal substrate; in this regard, the graded substrate shows a clear promise from a perspective of heat transfer enhancement.

Figure 9.20c presents the area of coverage created by the footprints of the drops on the substrate, as a function of time. As soon as the virgin substrate is exposed to vapor flux, direct condensation is initiated, and the area coverage of drops increases rapidly. Later, coalescence dominates direct condensation, eventually leading to droplet criticality. The cycle is then established, and the area coverage tends to stabilize. On a horizontal substrate, only a fall-off criticality is possible while on a graded substrate, a slide-off criticality is usually achieved first. During sliding motion, a droplet may fall-off in transit due to increase in its weight. A quasi-steady-state is eventually reached, after which the area coverage oscillates around an average value.

Results shown in Figs. 9.17, 9.18, 9.19, and 9.20 reveal that area coverage is smaller for the graded surface, making the exposed area greater than the other two surfaces considered. Further, drop instability in the form of a slide-off event is
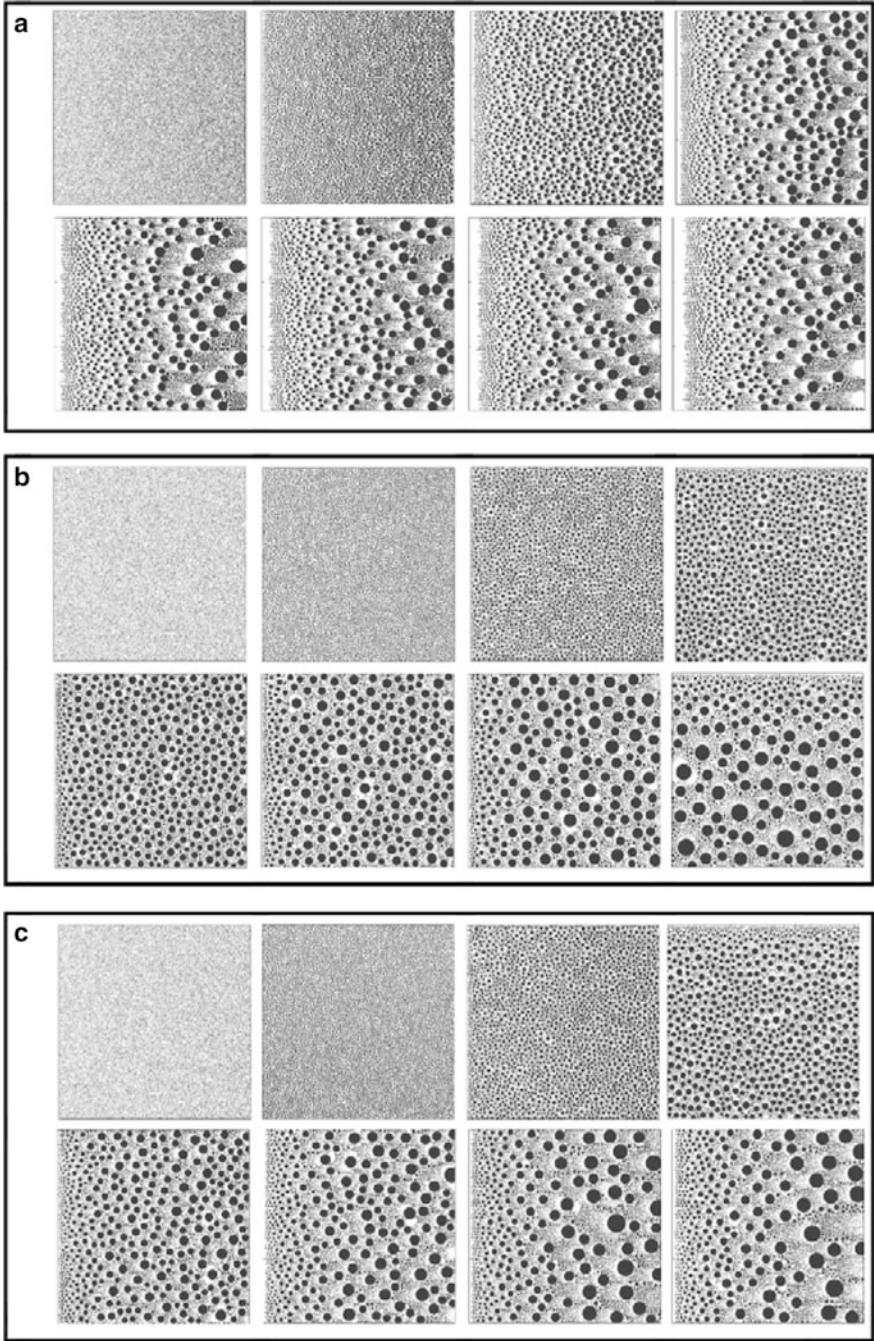
Fig. 9.19 Drop distribution condensed water vapor underneath a horizontal substrate with a wettability gradient. Contact angles are (**a**) 130° and 90°, (**b**) 130° and 100°, and (**c**) 130° and 120°
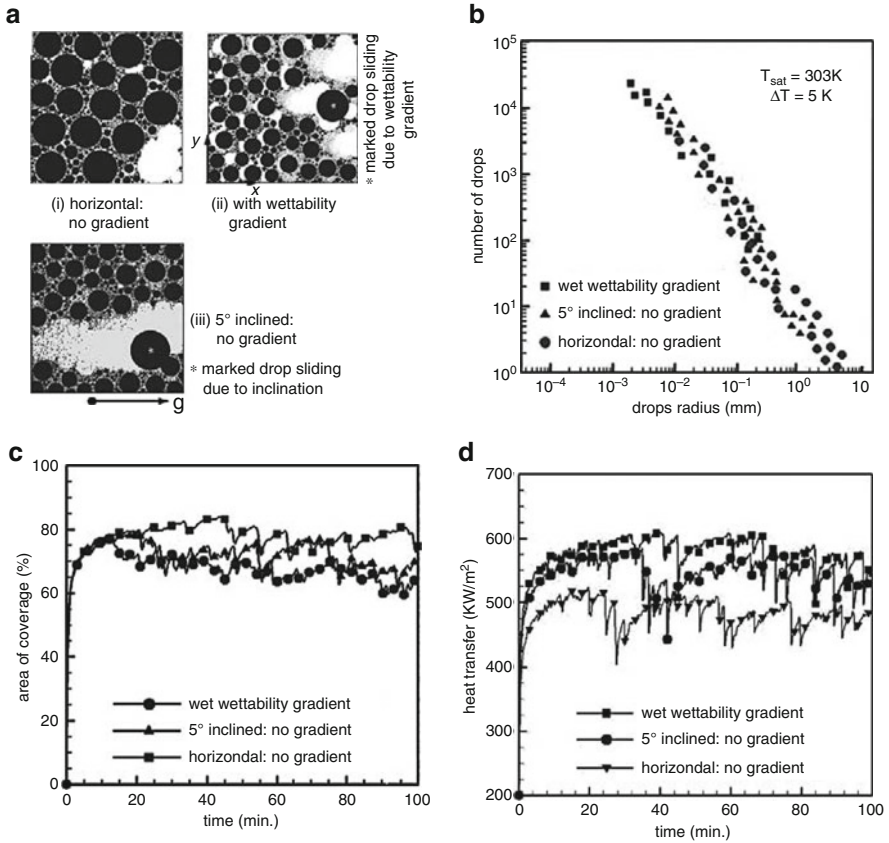
Fig. 9.20 Dropwise condensation of water vapor at 303 K with 5 K subcooling underneath surfaces of various textures. (**a**) Drop distribution underneath various substrates soon after instability. (**b**) Number of drops as a function of drop radius, just before the largest drop leaves the surface. (**c**) Effect of the choice of the substrate on percentage area of coverage. (**d**) Variation of heat transfer coefficient with time over various substrates

relatively early on the graded surface. As a direct consequence, heat transfer coefficient is expected to be higher for a surface with variable wettability. Heat transfer rates computed on these surfaces were found to be 450 (horizontal), 520 (inclined), and 540 (graded horizontal) in units of kW/m^2, with a subcooling of 5 K and a condensation temperature of 303 K.

9.2   Closure

Water vapor condensation underneath horizontal, inclined, and wettability gradient surfaces have been studied by numerical simulation. The effects of contact angle, its hysteresis, inclination of the substrate, thermophysical properties of the working fluid, and saturation temperature of condensation are investigated. Based on numerical data, heat transfer coefficients of water vapor condensation are correlated. In order, the horizontal, inclined, and the graded surface experience (a) larger to smaller drop sizes, (b) longer to shorter cycle times, and (c) lower to higher heat transfer coefficients. Validation of the mathematical model against experiments is discussed in the following chapter.